Adaptive Control of Nonlinear Underwater Robotic Systems

Thor I. Fossen

Department of Engineering Cybernetics
Norwegian Institute of Technology
N-7034 Trondheim, Norway

Svein I. Sagatun

Division of Engineering Cybernetics
Norwegian Institute of Technology
N-7034 Trondheim, Norway

Abstract

The problem of controlling underwater mobile robots in 6 degrees of freedom (DOF) is addressed. Uncertainties in the input matrix due to partly known nonlinear thruster characteristics are modelled as multiplicative input uncertainty. This paper proposes two methods to compensate for the model uncertainties: (1) an adaptive passivity-based control scheme and (2) deriving a hybrid (adaptive and sliding) controller. The hybrid controller consists of a switching term which compensates for uncertainties in the input matrix and an on-line parameter estimation algorithm. Global stability is ensured by applying Barbalat's Lyapunov-like lemma. The hybrid controller is simulated for the horizontal motion of the Norwegian Experimental Remotely Operated Vehicle (NEROV).

1 Introduction

Non-destructive testing of underwater structures require high performance manoeuvres of underwater mobile robots within and close to underwater installations. Until recently, remotely operated vehicles (ROVs) have been used as a platform for underwater robot manipulators. Now it is planned to use fully or partially autonomous underwater vehicles (AUVs) in such operations. This imposes stricter requirements on the control system particularly when macro-micro control i.e. control of the combined motion between the AUV and robot manipulator is of interest. The schemes presented in this paper are intended for the macro-micro control of such systems.

The underwater vehicle dynamics is strongly coupled and highly nonlinear. In robotics, adaptive controllers have given high performance for nonlinear systems [1, 6, 8, 11]. When designing controllers for underwater robotic systems, it is necessary to compensate for model features such as nonlinear dynamics, nonlinear kinematics and nonlinearities due to hysteresis, actuator dead-zones and partly known thruster characteristics. Precise knowledge of the dynamic parameters are required. This suggests a robust adaptive control scheme. This paper proposes two globally stable adaptive controllers for underwater robotic systems. Input uncertainties due to imprecise thruster characteristics are discussed in depth.

The paper is outlined as follows. Section 2 describes the equations of motion for underwater vehicles. Section 3 discusses adaptive passivity-based control of underwater vehicles. Hybrid adaptive control of underwater robotic systems with uncertainties in the input matrix is examined in Section 4, while the simulation study is presented in Section 5. Our conclusions are given at the end of the paper.

2 ROV Equations of Motion

It is convenient to define the ROV state vectors according to the Society of Naval Architects and Marine Engineers (SNAME) notation. The body-fixed linear and angular velocity vector in surge, sway, heave, roll, pitch and yaw, is defined as: $\dot{\boldsymbol{q}} = (u, v, w, p, q, r)^T$, where $\boldsymbol{q}$ is a virtual vector. The corresponding earth-fixed position and Euler angle vector is defined as: $\boldsymbol{x} = (x, y, z, \phi, \theta, \psi)^T$.

2.1 ROV Dynamics and Kinematics

The dynamic behavior of an underwater vehicle is described through Newton's laws of linear and angular momentum. The equations of motion of such vehicles are highly nonlinear and coupled due to hydrodynamic added mass, lift and drag forces, which are acting on the vehicle. It is convenient to write the nonlinear underwater vehicle equations of motion [4] as:

$$\boldsymbol{M}\ddot{\boldsymbol{q}} + \boldsymbol{C}(\dot{\boldsymbol{q}})\dot{\boldsymbol{q}} + \boldsymbol{D}(\dot{\boldsymbol{q}})\dot{\boldsymbol{q}} + \boldsymbol{g}(\boldsymbol{x}) = \boldsymbol{\tau} \quad (1)$$

$$\dot{\boldsymbol{x}} = \boldsymbol{J}(\boldsymbol{x})\dot{\boldsymbol{q}} \quad (2)$$

where $\boldsymbol{\tau} \in \Re^n$ is a vector of control forces and moments, $\boldsymbol{q} \in \Re^n$ and $\boldsymbol{x} \in \Re^n$. $\boldsymbol{M}$ is an $n \times n$ inertia matrix, $\boldsymbol{C}(\dot{\boldsymbol{q}})$ is an $n \times n$ matrix of centrifugal and Coriolis terms, $\boldsymbol{D}(\dot{\boldsymbol{q}})$ is an $n \times n$ dissipative matrix of hydrodynamic damping terms and $\boldsymbol{g}(\boldsymbol{x})$ is an $n \times 1$ vector including restoring forces and moments. These terms are described more closely in [3, 4, 5]. The vehicle's flight path relative to the earth-fixed reference frame is given by the kinematic equation Eq. 2. Hence, $\boldsymbol{J}(\boldsymbol{x})$ can be interpreted as an $n \times n$ kinematic transformation matrix, usually function of the Euler angles: ϕ, θ and ψ.

2.2 Thruster Hydrodynamics

Small underwater vehicles usually operate over a considerable speed range with no specific speed dominating. For such vehicles the performance of the ducted thrusters will be a function of advance velocity V_A at the propeller, propeller revolutions n and propeller diameter D. The non-dimensional open water characteristics [2], are defined in terms of the open water advance coefficient J_o:

$$J_o = \frac{V_A}{nD}$$

The non-dimensional thrust and torque coefficients K_T and K_Q and thruster open water efficiency η_o are defined as:

$$K_T = \frac{T}{\rho n|n|D^4} \quad ; \quad K_Q = \frac{Q}{\rho n|n|D^5} \quad ; \quad \eta_o = \frac{J_o}{2\pi} \cdot \frac{K_T}{K_Q}$$

where ρ is the water density and T and Q are the propeller thrust and torque, respectively. By carrying out an open water test a unique curve, where J_o is plotted against K_T and K_Q, is obtained for each propeller. A typical plot is shown in Fig. 1. For the NEROV thruster an open water test was performed in the towing tank at the Norwegian Marine Technology Research Institute in Trondheim. The results from this test are shown in Fig. 2.

In Figure 3, the thruster forces are plotted versus the speed of advance V_A and the propeller revolution n.

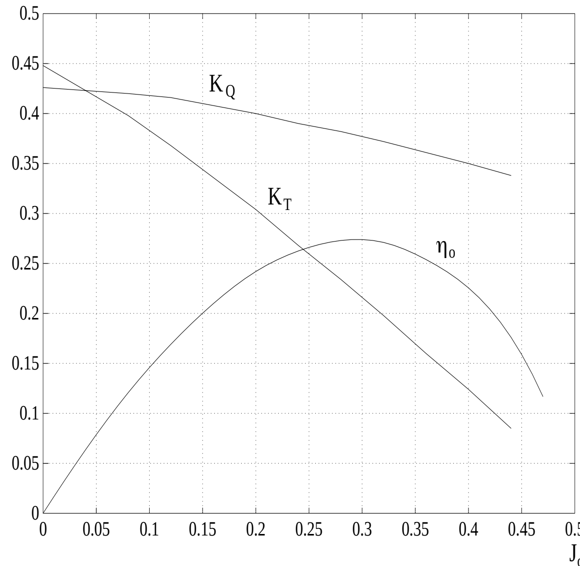

Figure 1: Non-dimensional thruster characteristics K_T, K_Q and η_o as a function of positive advance coefficient J_o (ahead direction).

When designing the control system the nonlinearities imposed by the propulsion system should be compensated. The thruster force can be approximated as:

$$T \approx \hat{b}(J_o)\ n|n| \ \text{ where } \ \hat{b}(J_o) = \hat{K}_T(J_o)\ \rho D^4$$

Here $\hat{K_T}$ is the estimate of the non-dimensional thrust coefficient. For positive J_o, Fig. 2 suggests that $\hat{K}_T$ can be linearly interpolated as:

$$\hat{K}_T(J_o) \approx \alpha + \beta\ J_o$$

where α and β are two constants. The advance velocity at the propeller V_A is related to the vehicle's speed V by the wake fraction number w as:

$$V_A = (1 - w)V$$

If the vehicle's velocity V_k is measured at time k, the advance coefficient $J_{o,\,k}$ can be approximated as:

$$J_{o,\,k} \approx \frac{(1 - w)V_k}{n_{k-1}D}$$

Here n_{k-1} is the measurement of the propeller revolution at time $k - 1$. A control input vector $\boldsymbol{u} = (u_1, ..., u_p)^T$ with elements:

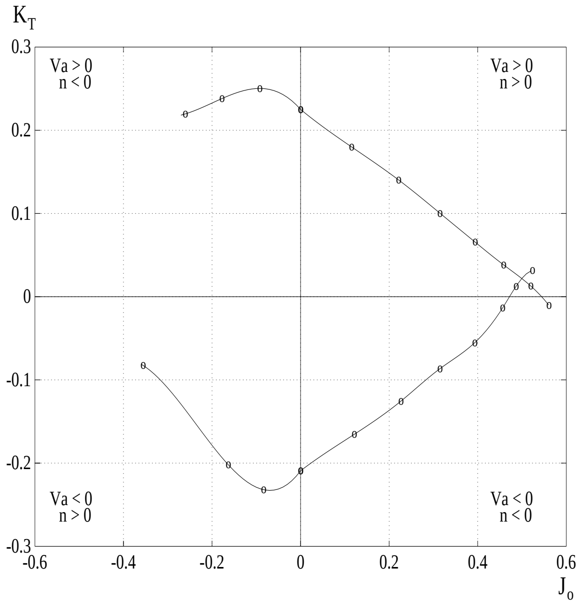

Figure 2: Non-dimensional experimental thruster coefficient K_T versus negative and positive advance coefficient J_o for the NEROV vehicle.

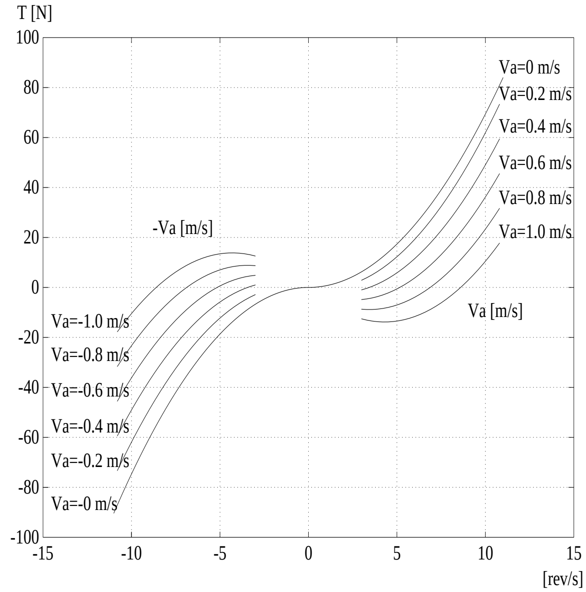

Figure 3: Thruster force T $[N]$ as a function of propeller revolutions n $[rev/min]$ for different speeds of advance V_A $[m/s]$ (positive advance coefficient J_o).

$$u_j = n_j|n_j| \qquad \Longleftrightarrow \qquad n_j = sgn(u_j)\,\sqrt{|u_j|}$$

where n_j is the propeller revolution of thruster j and sgn is signum function, shows that the elements in the input matrix $\boldsymbol{B}$ can be expressed as:

$$B_{ij}(\dot{\boldsymbol{q}}) \approx \hat{b}_j(J_o) \;\;,\;\; i = 1..n, \;\; j = 1..p$$

Here $\hat{b}_j$ is the nonlinear approximation corresponding to thruster input $u_j = n_j|n_j|$. As a result of this, the thruster force and moment vector $\boldsymbol{\tau}$ in Eq. 1 can be written as:

$$\boldsymbol{\tau} = \boldsymbol{B}(\dot{\boldsymbol{q}})\boldsymbol{u} \quad \text{where} \quad u_i = n_i|n_i| \;\;,\;\; i = 1..p$$

where $\boldsymbol{B}$ is the vehicle's input matrix. The uncertainties in the experimental data suggest an adaptive control scheme. Open water tests can be used as *a priori* information for the adaptive parameter update law.

2.3 Optimal Distribution of Propulsion and Control Forces

For underwater vehicles where $p \geq n$, i.e. equal or more control inputs than controllable DOF, it is possible to find an optimal distribution of thruster forces and also control surface forces, for each DOF. Consider the energy cost function:

$$\text{Min } J = \frac{1}{2}\boldsymbol{u}^T\boldsymbol{W}\boldsymbol{u} \qquad \text{subject to} \qquad \boldsymbol{\tau} = \boldsymbol{B}\boldsymbol{u}$$

where $\boldsymbol{W}$ is a positive definite, usually diagonal energy weighting matrix. For underwater vehicles which have both control surfaces and thrusters, the elements in W should be selected such that the use of control surfaces are much more inexpensive than the use of thrusters i.e. providing a means of saving battery energy. If $\boldsymbol{B}\boldsymbol{W}^{-1}\boldsymbol{B}^T$ is nonsingular, it is straightforward to show that:

$$\boldsymbol{\tau} = \boldsymbol{B}_W^+\,\boldsymbol{u} \;\text{ where }\; \boldsymbol{B}_W^+ = \boldsymbol{W}^{-1}\boldsymbol{B}^T(\boldsymbol{B}\boldsymbol{W}^{-1}\boldsymbol{B}^T)^{-1}$$

minimizes the energy cost function J. In the case when all inputs are equality weighted, i.e. $\boldsymbol{W} = \boldsymbol{I}$, the generalized inverse is simply:

$$\boldsymbol{B}^+ = \boldsymbol{B}^T(\boldsymbol{B}\boldsymbol{B}^T)^{-1}$$

Notice that for the square case: $\boldsymbol{B}^+ = \boldsymbol{B}^{-1}$.

3 Adaptive Control of Underwater Robotic Systems

We will restrict our treatment to systems with equal or more control inputs than controllable DOF, i.e. $p \geq n$.

3.1 B known

If $\boldsymbol{B}$ is known, the control input can be calculated as $\boldsymbol{u} = \boldsymbol{B}^{+}\boldsymbol{\tau}$. Let us again consider the underwater vehicle equations of motion, Eq. 1 and Eq. 2, which can be written as:

$$\boldsymbol{M}^*(\boldsymbol{x})\ddot{\boldsymbol{x}} + \boldsymbol{C}^*(\boldsymbol{x},\dot{\boldsymbol{x}})\dot{\boldsymbol{x}} + \boldsymbol{D}^*(\boldsymbol{x},\dot{\boldsymbol{x}})\dot{\boldsymbol{x}} + \boldsymbol{g}^*(\boldsymbol{x}) = \boldsymbol{J}^{-T}(\boldsymbol{x})\boldsymbol{\tau}$$

where

$$\begin{aligned}
\boldsymbol{M}^*(\boldsymbol{x}) &= \boldsymbol{J}^{-T}\boldsymbol{M}\boldsymbol{J}^{-1} \\
\boldsymbol{C}^*(\boldsymbol{x},\dot{\boldsymbol{x}}) &= \boldsymbol{J}^{-T}\left[\boldsymbol{C} - \boldsymbol{M}\boldsymbol{J}^{-1}\dot{\boldsymbol{J}}\right]\boldsymbol{J}^{-1} \\
\boldsymbol{D}^*(\boldsymbol{x},\dot{\boldsymbol{x}}) &= \boldsymbol{J}^{-T}\boldsymbol{D}\boldsymbol{J}^{-1} \\
\boldsymbol{g}^*(\boldsymbol{x}) &= \boldsymbol{J}^{-T}\boldsymbol{g}
\end{aligned}$$

Assume the desired trajectory: $\ddot{\boldsymbol{x}}_d$, $\dot{\boldsymbol{x}}_d$ and $\boldsymbol{x}_d$ to be bounded. Let $\tilde{\boldsymbol{x}} = \boldsymbol{x} - \boldsymbol{x}_d$ be the tracking error and $\tilde{\boldsymbol{\theta}}$ be the parameter error vector. [8, 9] suggest defining a measure of tracking $\boldsymbol{s}$ as:

$$\boldsymbol{s} = \dot{\tilde{\boldsymbol{x}}} + \lambda\tilde{\boldsymbol{x}} \tag{3}$$

where λ is a strictly positive constant which may be interpreted as the control bandwidth. It is convenient to rewrite Eq. 3 as:

$$\boldsymbol{s} = \dot{\boldsymbol{x}} - \dot{\boldsymbol{x}}_r \quad \text{where} \quad \dot{\boldsymbol{x}}_r = \dot{\boldsymbol{x}}_d - \lambda\tilde{\boldsymbol{x}}$$

To prove global stability [9] suggests using a Lyapunov-like function:

$$V(\boldsymbol{s},\tilde{\boldsymbol{\theta}},t) = \frac{1}{2}\boldsymbol{s}^T\boldsymbol{M}^*\boldsymbol{s} + \frac{1}{2}\tilde{\boldsymbol{\theta}}^T\boldsymbol{\Gamma}\tilde{\boldsymbol{\theta}}$$

where $\boldsymbol{\Gamma}$ is a symmetric positive definite weighting matrix of appropriate dimension. Differentiating V with respect to time and using the skew symmetric property $\dot{\boldsymbol{x}}^T(\dot{\boldsymbol{M}}^* - 2\boldsymbol{C}^*)\,\dot{\boldsymbol{x}} = 0$ yields:

$$\begin{aligned}
\dot{V} = &-\boldsymbol{s}^T\boldsymbol{D}^*\boldsymbol{s} + \dot{\tilde{\boldsymbol{\theta}}}^T\boldsymbol{\Gamma}\tilde{\boldsymbol{\theta}} \\
&+\boldsymbol{s}^T(\boldsymbol{J}^{-T}\boldsymbol{\tau} - \boldsymbol{M}^*\ddot{\boldsymbol{x}}_r - \boldsymbol{C}^*\dot{\boldsymbol{x}}_r - \boldsymbol{D}^*\dot{\boldsymbol{x}}_r - \boldsymbol{g}^*)
\end{aligned}$$

[4] defines a virtual vector $\dot{\boldsymbol{q}}_r$ which satisfies the transformation:

$$\dot{\boldsymbol{x}}_r = \boldsymbol{J}(\boldsymbol{x})\,\dot{\boldsymbol{q}}_r$$

Hence, the virtual reference vectors $\dot{\boldsymbol{q}}_r$ and $\ddot{\boldsymbol{q}}_r$ can be calculated as:

$$\begin{aligned}
\dot{\boldsymbol{q}}_r &= \boldsymbol{J}^{-1}(\boldsymbol{x})\dot{\boldsymbol{x}}_r \\
\ddot{\boldsymbol{q}}_r &= \boldsymbol{J}^{-1}(\boldsymbol{x})\ddot{\boldsymbol{x}}_r - \boldsymbol{J}^{-1}(\boldsymbol{x})\dot{\boldsymbol{J}}(\boldsymbol{x})\boldsymbol{J}^{-1}(\boldsymbol{x})\dot{\boldsymbol{x}}_r
\end{aligned}$$

We now notice that the unknown terms $\boldsymbol{M}^*, \boldsymbol{C}^*, \boldsymbol{D}^*$ and $\boldsymbol{g}^*$ can be parameterized as:

$$\boldsymbol{M}^*\ddot{\boldsymbol{x}}_r + \boldsymbol{C}^*\dot{\boldsymbol{x}}_r + \boldsymbol{D}^*\dot{\boldsymbol{x}}_r + \boldsymbol{g}^* =$$

$$\boldsymbol{J}^{-T}\left[\boldsymbol{M}\ddot{\boldsymbol{q}}_r + \boldsymbol{C}\dot{\boldsymbol{q}}_r + \boldsymbol{D}\dot{\boldsymbol{q}}_r + \boldsymbol{g}\right] = \boldsymbol{J}^{-T}\boldsymbol{\Phi}(\boldsymbol{x},\dot{\boldsymbol{q}},\dot{\boldsymbol{q}}_r,\ddot{\boldsymbol{q}}_r)\,\boldsymbol{\theta}$$

where $\boldsymbol{\theta}$ is an unknown parameter vector and $\boldsymbol{\Phi}$ is a known regressor matrix of appropriate dimensions. We have here assumed that the terms $\boldsymbol{M}^*$, $\boldsymbol{C}^*$, $\boldsymbol{D}^*$ and $\boldsymbol{g}^*$ are linear in their parameters. By using $\boldsymbol{q}_r$ instead of $\boldsymbol{x}_r$ in the parameterization, the transformation matrix $\boldsymbol{J}(\boldsymbol{x})$ is avoided in the expression for the regressor matrix. This yields:

$$\dot{V} = -\boldsymbol{s}^T\boldsymbol{D}^*\boldsymbol{s} + \boldsymbol{s}^T\boldsymbol{J}^{-T}(\boldsymbol{\tau} - \boldsymbol{\Phi}\,\boldsymbol{\theta}) + \dot{\tilde{\boldsymbol{\theta}}}^T\boldsymbol{\Gamma}\tilde{\boldsymbol{\theta}} \tag{4}$$

Let the control law be:

$$\boldsymbol{\tau} = \boldsymbol{\Phi}\,\hat{\boldsymbol{\theta}} - \boldsymbol{J}^T\boldsymbol{K}_D\boldsymbol{s} \tag{5}$$

where $\hat{\boldsymbol{\theta}}$ is the estimated parameter vector and $\boldsymbol{K}_D$ is a symmetric positive definite design matrix of appropriate. Then, the parameter update law:

$$\dot{\hat{\boldsymbol{\theta}}} = -\boldsymbol{\Gamma}^{-1}\boldsymbol{\Phi}^T(\boldsymbol{x},\dot{\boldsymbol{q}},\dot{\boldsymbol{q}}_r,\ddot{\boldsymbol{q}}_r)\boldsymbol{J}^{-1}(\boldsymbol{x})\,\boldsymbol{s}$$

yields:

$$\dot{V} = -\boldsymbol{s}^T(\boldsymbol{K}_D + \boldsymbol{D}^*)\boldsymbol{s} \leq 0$$

This is due to the fact that the dissipative term $\boldsymbol{D} > 0$ implies that $\boldsymbol{D}^* = \boldsymbol{J}^{-T}\boldsymbol{D}\boldsymbol{J}^{-1} > 0$. Hence, Barbalat's Lyapunov-like lemma ensures that $\boldsymbol{s} \to 0$ and thus the tracking error vector $\tilde{\boldsymbol{x}} \to 0$.

3.2 B unknown.

The results in the previous section may be extended to underwater vehicles with multiplicative input uncertainty i.e.

$$\boldsymbol{B}(\dot{\boldsymbol{q}}) = (\boldsymbol{I}+\boldsymbol{\Delta})\boldsymbol{B}_o(\dot{\boldsymbol{q}}) \quad , \quad \boldsymbol{\Delta} \in \{\boldsymbol{\Delta} : \overline{\sigma}(\boldsymbol{\Delta}) < 1\} \tag{6}$$

where $\boldsymbol{\Delta}$ is an unknown $n \times n$ perturbation matrix, $\overline{\sigma}(\boldsymbol{\Delta})$ is the maximum singular value of $\boldsymbol{\Delta}$ and $\boldsymbol{B}_o(\dot{\boldsymbol{q}})$ is a known $n \times p$ matrix found from experiments. Substituting Eq. 6 into Eq. 4 yields:

$$\dot{V} = -\boldsymbol{s}^T\boldsymbol{D}^*\boldsymbol{s} + \boldsymbol{s}^T\boldsymbol{J}^{-T}\left[(\boldsymbol{I}+\boldsymbol{\Delta})\boldsymbol{B}_o\boldsymbol{u} - \boldsymbol{\Phi}\,\boldsymbol{\theta}\right] + \dot{\tilde{\boldsymbol{\theta}}}^T\Gamma\tilde{\boldsymbol{\theta}}$$

Defining:

$$\boldsymbol{M}_\Delta = (\boldsymbol{I}+\boldsymbol{\Delta})^{-1}\boldsymbol{M} \qquad \boldsymbol{D}_\Delta = (\boldsymbol{I}+\boldsymbol{\Delta})^{-1}\boldsymbol{D}$$
$$\boldsymbol{C}_\Delta = (\boldsymbol{I}+\boldsymbol{\Delta})^{-1}\boldsymbol{C} \qquad \boldsymbol{g}_\Delta = (\boldsymbol{I}+\boldsymbol{\Delta})^{-1}\boldsymbol{g}$$

and

$$\boldsymbol{M}_\Delta\ddot{\boldsymbol{q}}_r + \boldsymbol{C}_\Delta\dot{\boldsymbol{q}}_r + \boldsymbol{D}_\Delta\dot{\boldsymbol{q}}_r + \boldsymbol{g}_\Delta = \boldsymbol{\Phi}_\Delta(\boldsymbol{x},\dot{\boldsymbol{q}},\dot{\boldsymbol{q}}_r,\ddot{\boldsymbol{q}}_r)\,\boldsymbol{\theta}$$

$\dot{V}$ may be written as:

$$\dot{V} = -\boldsymbol{s}^T\boldsymbol{D}^*\boldsymbol{s} + \boldsymbol{s}^T\boldsymbol{J}^{-T}(\boldsymbol{I}+\boldsymbol{\Delta})\left[\boldsymbol{B}_o\boldsymbol{u} - \boldsymbol{\Phi}_\Delta\boldsymbol{\theta}\right] + \dot{\tilde{\boldsymbol{\theta}}}^T\boldsymbol{\Gamma}\tilde{\boldsymbol{\theta}}$$

Taking the control law to be:

$$\boldsymbol{u} = \boldsymbol{B}_o^+\left[\boldsymbol{\Phi}_\Delta\,\hat{\boldsymbol{\theta}} - \boldsymbol{J}^T\boldsymbol{K}_D\boldsymbol{s}\right] \tag{7}$$

where $\boldsymbol{B}_o^+$ is a generalized inverse, the adaption law:

$$\dot{\hat{\boldsymbol{\theta}}} = -\boldsymbol{\Gamma}^{-1}\boldsymbol{\Phi}_\Delta^T(\boldsymbol{x},\dot{\boldsymbol{q}},\dot{\boldsymbol{q}}_r,\ddot{\boldsymbol{q}}_r)\boldsymbol{J}^{-1}(\boldsymbol{x})\,\boldsymbol{s}$$

yields:

$$\dot{V} = -\boldsymbol{s}^T\left[\boldsymbol{D}^* + \boldsymbol{J}^{-T}(\boldsymbol{I}+\boldsymbol{\Delta})\boldsymbol{J}^T\boldsymbol{K}_D\right]\boldsymbol{s} \le 0$$

where we have used the fact that $\overline{\sigma}(\boldsymbol{\Delta}) < 1$ implies that $(\boldsymbol{I}+\boldsymbol{\Delta}) > 0$ and thus:

$$\boldsymbol{J}^{-T}(\boldsymbol{I}+\boldsymbol{\Delta})\boldsymbol{J}^T > 0$$

i.e. positiveness of a matrix is invariant of scaling. As in the previous case, Barbalat's lemma implies that $\boldsymbol{s} \to 0$ and thus $\tilde{\boldsymbol{x}} \to 0$.

4 Hybrid Adaptive Control

In this section we will derive a hybrid (adaptive and sliding) control scheme which compensates for the uncertainty in the input matrix by adding a discontinuous term to the existing adaptive control law. Previous work on sliding mode control of underwater vehicles [12] does not compensate for the time-varying behaviour of the control input matrix due to the thruster hydrodynamics, i.e. $\boldsymbol{\tau} = \boldsymbol{B}(\dot{\boldsymbol{q}})\boldsymbol{u}$. In the following, it is convenient to define the operators:

$$\begin{aligned} |\,\boldsymbol{x}\,| &= [\,|\,x_1\,|, |\,x_2\,|, ..., |\,x_n\,|\,]^T \\ sgn(\boldsymbol{x}) &= [sgn(x_1), sgn(x_2), ..., sgn(x_n)]^T \\ \boldsymbol{x} .\!\times \boldsymbol{y} &= [x_1\,y_1, x_2\,y_2, ..., x_n\,y_n]^T \end{aligned}$$

4.1 B unknown

Let us again consider an underwater vehicle in 6 DOF. Assume that the thruster configuration matrix $\boldsymbol{B}$ satisfies a multiplicative uncertainty:

$$\boldsymbol{B}(\dot{\boldsymbol{q}}) = (\boldsymbol{I}+\boldsymbol{\Delta})\boldsymbol{B}_o(\dot{\boldsymbol{q}}) \quad , \quad |\Delta_{ij}| \le U_{ij} \tag{8}$$

This yields the following expression for $\dot{V}$, c.f. Eq. 4:

$$\dot{V} = -\boldsymbol{s}^T\boldsymbol{D}^*\boldsymbol{s} + \boldsymbol{s}^T\boldsymbol{J}^{-T}\left[(\boldsymbol{I}+\boldsymbol{\Delta})\boldsymbol{B}_o\boldsymbol{u} - \boldsymbol{\Phi}\,\boldsymbol{\theta}\right] + \dot{\tilde{\boldsymbol{\theta}}}^T\boldsymbol{\Gamma}\tilde{\boldsymbol{\theta}}$$

Let the control law be:

$$\boldsymbol{u} = \boldsymbol{B}_o^+\left[\boldsymbol{\Phi}\,\hat{\boldsymbol{\theta}} - \boldsymbol{J}^T\boldsymbol{K}_D\boldsymbol{s} - \boldsymbol{k} .\!\times sgn(\boldsymbol{J}^{-1}\boldsymbol{s})\right] \tag{9}$$

Here we have added a switching term $\boldsymbol{k} .\!\times sgn(\boldsymbol{J}^{-1}\boldsymbol{s})$ to compensate for the uncertainty in the $\boldsymbol{B}$ matrix. Conditions on the non-negative switching gain vector $\boldsymbol{k}$ are found by selecting the adaption law as:

$$\dot{\hat{\boldsymbol{\theta}}} = -\boldsymbol{\Gamma}^{-1}\boldsymbol{\Phi}^T(\boldsymbol{x},\dot{\boldsymbol{q}},\dot{\boldsymbol{q}}_r,\ddot{\boldsymbol{q}}_r)\,\boldsymbol{J}^{-1}(\boldsymbol{x})\,\boldsymbol{s}$$

which implies that $\dot{V}$ may be written as:

$$\begin{aligned} \dot{V} = -\boldsymbol{s}^T(\boldsymbol{D}^* + \boldsymbol{K}_D)\boldsymbol{s} + (\boldsymbol{J}^{-1}\boldsymbol{s})^T\Big[\boldsymbol{\Delta}\,(\boldsymbol{\Phi}\hat{\boldsymbol{\theta}} \\ -\boldsymbol{J}^T\boldsymbol{K}_D\boldsymbol{s}) - (\boldsymbol{I}+\boldsymbol{\Delta})\,\boldsymbol{k} .\!\times sgn(\boldsymbol{J}^{-1}\boldsymbol{s})\Big] \end{aligned}$$

The particular choice $k_i \ge k'_i \quad \forall\, i$ where $\boldsymbol{k}'$ satisfies:

$$(\boldsymbol{I} - \overline{\boldsymbol{U}})\,\boldsymbol{k}' = \boldsymbol{U}\,|\,\boldsymbol{\Phi}\,\hat{\boldsymbol{\theta}} - \boldsymbol{J}^T\boldsymbol{K}_D\boldsymbol{s}\,| + \boldsymbol{\eta} \quad , \quad \eta_i > 0$$

where the elements U_{ij} are defined in Eq. 8 and the matrix $\overline{\boldsymbol{U}}$ is defined as:

$$\overline{\boldsymbol{U}} = \begin{bmatrix} U_{11} & -U_{12} & \dots & -U_{1n} \\ -U_{21} & U_{22} & & -U_{2n} \\ \vdots & & \ddots & \vdots \\ -U_{n1} & -U_{n2} & \dots & U_{nn} \end{bmatrix}$$

yields:

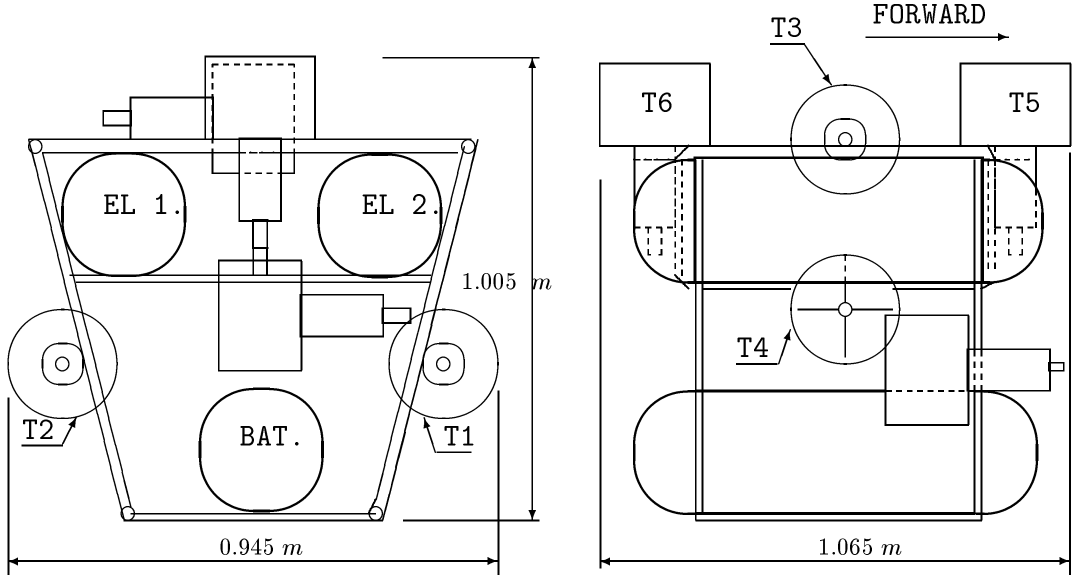

Figure 4: General arrangement of the NEROV vehicle.

$$\dot{V} \leq -\boldsymbol{s}^T(\boldsymbol{D}^* + \boldsymbol{K}_D)\boldsymbol{s} - \boldsymbol{\eta}^T|\boldsymbol{J}^{-1}\boldsymbol{s}| \leq 0$$

Applying Barbalat's lemma implies that $\boldsymbol{s} \rightarrow 0$ and thus $\boldsymbol{x} \rightarrow 0$. According to the Frobenius-Perron lemma [10], the existence of a unique $\boldsymbol{k}$ vector is guaranteed, namely:

$$\boldsymbol{k}' = (\boldsymbol{I} - \overline{\boldsymbol{U}})^{-1}\left[\boldsymbol{U} \mid \Phi\hat{\boldsymbol{\theta}} - \boldsymbol{J}^T\boldsymbol{K}_D\boldsymbol{s} \mid + \boldsymbol{\eta}\right]$$

Note, that the design matrix $\boldsymbol{K}_D$ directly accelerates the convergence rate. Chattering imposed by the discontinuous term $\boldsymbol{k} \;.\times\; sgn(\boldsymbol{J}^{-1}\boldsymbol{s})$ can be avoided by smoothing out the control law within boundary layers, [10].

5 Simulation Study

The simulation study is based on a simplified model of the Norwegian Experimental Remotely Operated Vehicle (NEROV). The NEROV vehicle is an autonomous underwater vehicle which is designed at the Division of Engineering Cybernetics at the Norwegian Institute of Technology. A brief sketch of the vehicle's general arrangement [7], is shown in Fig. 4. The vehicle is controllable in all 6 DOF. The propulsion system is based on 6 independent DC permanent magnet motors with propeller angular velocity measurements. The hybrid controller was simulated for the horizontal motion of the NEROV vehicle i.e. the coupled motion in surge, sway and yaw ($\dot{\boldsymbol{q}} = [u, v, r]^T$ and $\boldsymbol{x} = [x, y, \psi]^T$). The NEROV model was simply chosen as:

$$\boldsymbol{M} = \begin{bmatrix} 186 & 0 & 0 \\ 0 & 268 & 0 \\ 0 & 0 & 29 \end{bmatrix} \quad \boldsymbol{C} = \begin{bmatrix} 0 & 268r & 0 \\ -268r & 0 & 0 \\ 0 & 0 & 0 \end{bmatrix}$$

$$\boldsymbol{D} = \begin{bmatrix} 119 & 0 & 0 \\ 0 & 208 & 0 \\ 0 & 0 & 15 \end{bmatrix} \quad \boldsymbol{J} = \begin{bmatrix} \cos\psi & -\sin\psi & 0 \\ \sin\psi & \cos\psi & 0 \\ 0 & 0 & 1 \end{bmatrix}$$

$$\boldsymbol{B}_o = \begin{bmatrix} \hat{b} & 0 & 0 \\ 0 & \hat{b} & 0 \\ 0 & 0 & \hat{b} \end{bmatrix} \begin{bmatrix} 1 & 1 & 0 & 0 \\ 0 & 0 & -1 & 1 \\ -0.4 & 0.4 & 0 & 0 \end{bmatrix}$$

where $\hat{b} = \hat{K}_T \rho D^4$ and $\hat{K}_T$ is found from Fig. 2. The uncertainties in the thruster characteristics were modelled as a diagonal matrix Δ with diagonal elements [0.3 -0.5 0.4]. The initial values for the parameter estimates were chosen as zero and the sampling rate was set at 10 Hz. Fig. 5 shows the desired trajectories x_d, y_d and ψ_d and tracking errors $e_x = x - x_d$, $e_y = y - y_d$ and $e_\psi = \psi - \psi_d$ in surge, sway in yaw. The propeller angular velocities u_{1-4} were calculated from the hybrid control law Eq. 9. The control inputs are shown in the lower part of the figure. The simulations show that all tracking errors converge to zero.

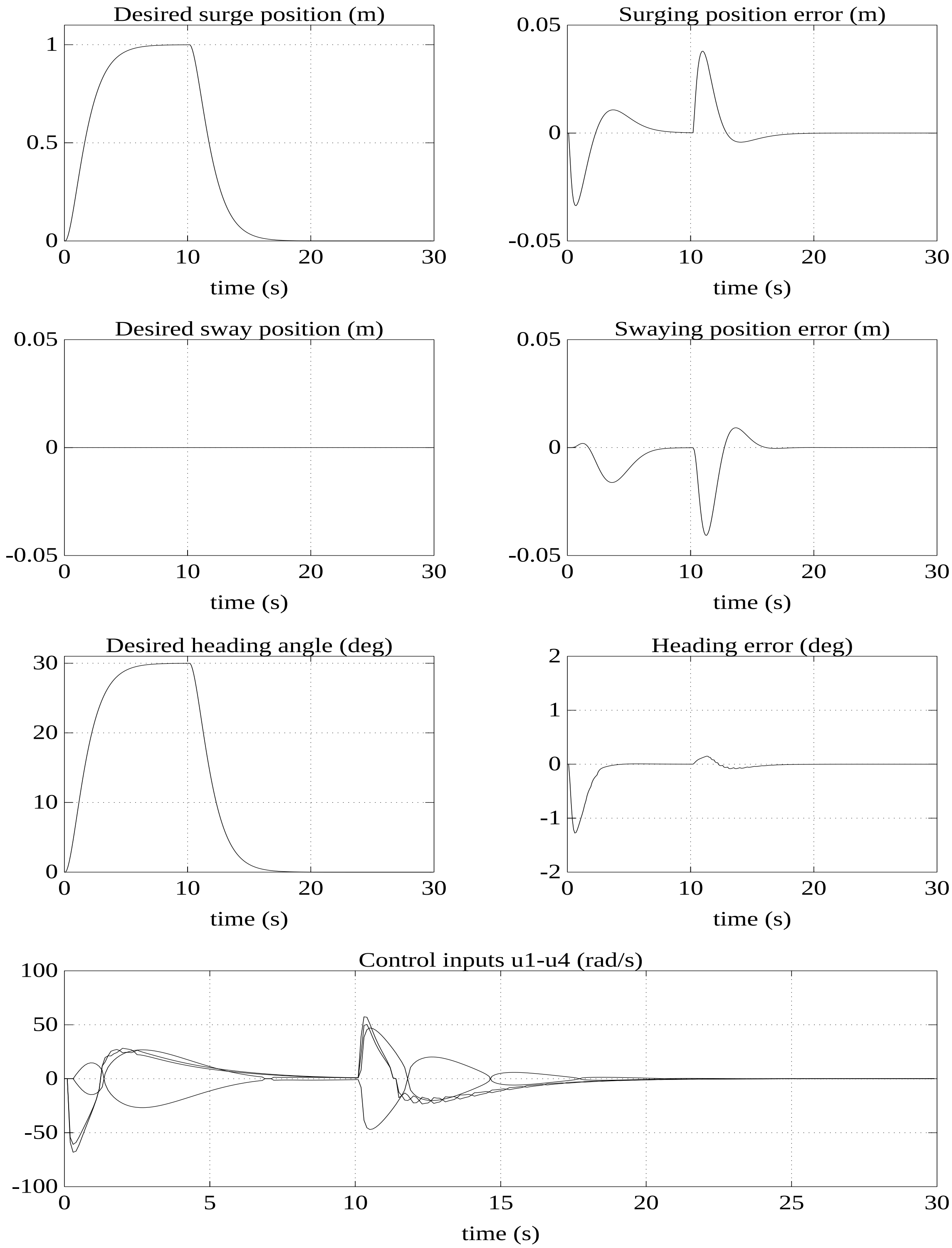

Figure 5: Desired trajectories (left), tracking errors (right) and control inputs (bottom) for the hybrid controller.

6 Conclusions

Two adaptive controllers for nonlinear robotic systems have been presented in this paper. The first controller is an extension of an adaptive passivity-based controller for robot manipulators and spacecrafts to nonlinear underwater robotic systems. The second scheme is a hybrid controller utilizing both the results from the adaptive controller and the theory of sliding mode control. Systems with input uncertainties are discussed in depth. The paper shows how an adaptive and hybrid (adaptive and sliding) controller can exploit the nonlinear thruster characteristics found from open water tests. The hybrid controller is simulated for the NEROV vehicle.

Acknowledgments

This work was partially sponsored by the Fulbright Foundation and the Royal Norwegian Council for Scientific and Industrial Research through the Center for Robotic Research at the Norwegian Institute of Technology. The authors are grateful to Erik Lehn at the Norwegian Marine Technology Research Institute and Bjørn Sortland at the Division of Marine Systems Design, NTH for their stimulating discussions and help with the open water tests of the NEROV thruster.

References

[1] J. J. Craig, P. Hsu and S. Sastry, "Adaptive Control of Mechanical Manipulators," *IEEE Int. Conf. on Robotics and Automation*, San Francisco, April, 1986.

[2] I. Dand and M. J. Every, "An Overview of the Hydrodynamics of Umbilical Cables and Vehicles", *SUBTECH' 83*, Paper No. 10.4., 1983.

[3] T. I. Fossen and J. G. Balchen, "Modelling and Nonlinear Self-Tuning Robust Trajectory Control of an Autonomous Underwater Vehicle," *Modelling, Identification and Control*, **MIC-9**, No. 4, pp. 165-177, 1988.

[4] T. I. Fossen, *Nonlinear Modelling and Control of Underwater Vehicles.* Dr. ing thesis, Division of Engineering Cybernetics, Norwegian Institute of Technology, September 1991.

[5] D. J. Lewis, J. M. Lipscombe and P. C. Thomasson, "The Simulation of Remotely Operated Vehicles," *in proceedings ROV'84*, pp. 245-251, 1984.

[6] N. Sadegh, and R. Horowitch, "Stability Analysis of an Adaptive Controller for Robotic Manipulators," *in proceedings IEEE Int. Conf. on Robotics and Automation*, Raleigh, North Carolina, 1987.

[7] S. I. Sagatun and T. I. Fossen. Design Study of The Norwegian Experimental Remotely Operated Vehicle. *Division of Engineering Cybernetics, Norwegian Institute of Technology*, Report no. 90-57-W, 1990.

[8] J. J. E. Slotine and W. Li, "Adaptive Manipulator Control: A Case Study," *in proceedings IEEE Int. Conference on Robotics and Automation*, pp. 1392-1401, 1987.

[9] J. J. E. Slotine and M. D. Di Benedetto, "Hamiltonian Adaptive Control of Spacecraft," *IEEE Trans. Automatic Control*, **AC-35**, No. 7, pp. 848-852, 1990.

[10] J. J. E. Slotine and W. Li, *Applied Nonlinear Control*, Prentice-Hall, 1990.

[11] M. W. Spong and R. Ortega, "On Adaptive Inverse Dynamics Control of Rigid Robots," *IEEE Trans. Automatic Control*, **AC-35**, No.1, pp. 92-95, 1990.

[12] D. R. Yoerger and J. J. E. Slotine, "Robust Trajectory Control of Underwater Vehicles," *IEEE Journal of Oceanic Engineering*, **OE-10**, No. 4, pp. 462-470, 1985.